Inhibition of the integrated stress response reverses cognitive deficits after traumatic brain injury

Austin Chou[a,b,1], Karen Krukowski[a,c,d,1], Timothy Jopson[a,c], Ping Jun Zhu[e], Mauro Costa-Mattioli[e], Peter Walter[f,g,2], and Susanna Rosi[a,b,c,d,2]

[a]Brain and Spinal Injury Center, University of California, San Francisco, CA 94143; [b]Neuroscience Graduate Program, University of California, San Francisco, CA 94143; [c]Department of Physical Therapy Rehabilitation Science, University of California, San Francisco, CA 94143, [d]Department of Neurological Surgery, University of California, San Francisco, CA 94143; [e]Department of Neuroscience, Memory and Brain Research Center, Baylor College of Medicine, Houston, TX 77030; [f]Department of Biochemistry and Biophysics, University of California, San Francisco, CA 94143; and [g]Howard Hughes Medical Institute, University of California, San Francisco, CA 94143

Contributed by Peter Walter, June 15, 2017 (sent for review May 10, 2017; reviewed by Cesar Borlongan and Nahum Sonenberg)

Traumatic brain injury (TBI) is a leading cause of long-term neurological disability, yet the mechanisms underlying the chronic cognitive deficits associated with TBI remain unknown. Consequently, there are no effective treatments for patients suffering from the long-lasting symptoms of TBI. Here, we show that TBI persistently activates the integrated stress response (ISR), a universal intracellular signaling pathway that responds to a variety of cellular conditions and regulates protein translation via phosphorylation of the translation initiation factor eIF2α. Treatment with ISRIB, a potent drug-like small-molecule inhibitor of the ISR, reversed the hippocampal-dependent cognitive deficits induced by TBI in two different injury mouse models—focal contusion and diffuse concussive injury. Surprisingly, ISRIB corrected TBI-induced memory deficits when administered weeks after the initial injury and maintained cognitive improvement after treatment was terminated. At the physiological level, TBI suppressed long-term potentiation in the hippocampus, which was fully restored with ISRIB treatment. Our results indicate that ISR inhibition at time points late after injury can reverse memory deficits associated with TBI. As such, pharmacological inhibition of the ISR emerges as a promising avenue to combat head trauma-induced chronic cognitive deficits.

brain trauma | memory deficits | translational control | eIF2α | hippocampus

Traumatic brain injury (TBI) represents a major mental health problem (1–4). Even a mild TBI can elicit cognitive deficits, including permanent memory dysfunction (2, 4). Moreover, TBI is one of the most predictive environmental risk factors for the development of Alzheimer's disease and other forms of dementia (5–9). Current treatments have focused primarily on reducing the risk of TBI incidence, immediate neurosurgical intervention, or broad behavioral rehabilitation (10–13). Despite posing a huge societal problem, there are currently no pharmacological treatment options for patients that suffer from TBI-induced cognitive deficits.

The integrated stress response (ISR) is an evolutionarily conserved pathway that controls cellular homeostasis and function (14). The central ISR regulatory step is the phosphorylation of the α-subunit of the eukaryotic translation initiation factor 2 (eIF2α) by a family of four eIF2α kinases (15, 16). Phosphorylation of eIF2α leads to inhibition of general protein synthesis, but also, to the translational up-regulation of a select subset of mRNAs (17, 18). In the brain, phosphorylation of eIF2α regulates the formation of long-term memory (19–21). Briefly, animals with reduced phosphorylation of eIF2α show enhanced long-term memory storage (19, 22–24), and increased phosphorylation of eIF2α in the brain prevents the formation of long-term memory (19, 24, 25).

Similar to other chronic cognitive disorders (21, 26), TBI leads to a persistent activation of the ISR. TBI induces eIF2α phosphorylation even in brain regions that are distal to the injury site (27, 28). However, the direct impact of ISR activation on chronic TBI-induced behavioral deficits remains unknown.

We recently discovered a potent (in-cell EC_{50} = 5 nM) drug-like small molecule ISRIB (ISR inhibitor) that reverses the translational effects induced by ISR-mediated eIF2α phosphorylation and readily permeates the blood–brain barrier (29). ISRIB binds to eIF2's guanine nucleotide exchange factor eIF2B and induces its dimerization (30, 31). ISRIB-induced dimerization increases eIF2B-mediated guanine nucleotide exchange and desensitizes eIF2B activity to inhibition by phosphorylated eIF2α (p-eIF2α). As such, it blunts the effects of eIF2α phosphorylation on translation initiation. Strong parallels between in vivo genetic and pharmacological experiments support the notion that ISRIB exerts all its effect on target by inhibiting the ISR induced by eIF2α phosphorylation (19, 32, 33).

We hypothesized that TBI-induced sustained eIF2α phosphorylation in the hippocampus, a brain region crucially involved in memory formation, could be a major contributor to the permanent cognitive dysfunction observed after TBI (34). To test this notion, we investigated whether treatment with ISRIB, several weeks postinjury, could remedy TBI-induced impairments in cognitive function and associated changes in synaptic function.

Results

TBI Induces Acute and Persistent Phosphorylation of eIF2α in the Hippocampus. To investigate whether TBI activates the ISR in the hippocampus, we induced focal contusion injury using

Significance

Traumatic brain injury (TBI) is a leading cause of long-term neurological disability and affects an ever-growing population. Currently, there are no effective treatments for patients suffering from chronic TBI-induced cognitive impairments. Here, we found that suppression of the integrated stress response (ISR) with a drug-like small-molecule inhibitor, ISRIB, rescued cognition in two TBI mouse models, even when administered weeks after injury. Consistent with the behavioral results, ISRIB restored long-term potentiation deficits observed in TBI mice. Our data suggest that targeting ISR activation could serve as a promising approach for the treatment of chronic cognitive dysfunction after TBI.

Author contributions: A.C., K.K., M.C.-M., P.W., and S.R. designed research; A.C., K.K., T.J., P.J.Z., and M.C.-M. performed research; A.C., K.K., P.J.Z., M.C.-M., P.W., and S.R. analyzed data; and A.C., K.K., M.C.-M., P.W., and S.R. wrote the paper.

Reviewers: C.B., Center of Excellence for Aging and Brain Repair, University of South Florida; and N.S., McGill University.

Conflict of interest statement: P.W. [University of California San Francisco (UCSF) employee] has a patent application for the invention of ISRIB. Rights to the invention have been licensed by UCSF to Calico.

Freely available online through the PNAS open access option.

[1]A.C. and K.K. contributed equally to this work.

[2]To whom correspondence may be addressed. Email: peter@walterlab.ucsf.edu or Susanna.Rosi@ucsf.edu.

This article contains supporting information online at www.pnas.org/lookup/suppl/doi:10.1073/pnas.1707661114/-/DCSupplemental.

controlled cortical impact in mice (34). This mouse model of TBI exhibits cognitive deficits similar to those commonly observed after contusion injuries in humans (35). Briefly, we surgically exposed the brain and induced a controlled impact injury with a pneumatic piston on the right parietal cortex above the hippocampus. Sham controls received the same surgery but without a TBI. We collected and processed the hippocampus ipsilateral to the injury to quantify p-eIF2α levels at 1 and 28 d postinjury (dpi) (Fig. 1*A*). The phosphorylation of eIF2α was significantly increased in the hippocampus of animals with TBI at 1 dpi (Fig. 1 *B* and *C*). Compared with sham controls, in mice with TBI, hippocampal p-eIF2α remained elevated even 28 d after injury (Fig. 1 *D* and *E*), indicating that TBI triggers a persistent activation of the ISR in the hippocampus.

ISRIB Rescues TBI-Induced Deficits in Spatial Learning and Memory Consolidation. Next, we investigated whether blockage of the TBI-induced ISR could reverse the learning and memory deficits in mice with TBI. To this end, we induced focal TBI (as described in *Materials and Methods*) and allowed animals to recover for 4 wk. We then evaluated hippocampal-dependent long-term memory storage using a radial arm water maze (RAWM) (34). In this forced-swim behavioral test, animals learned to locate a hidden platform in one of the eight arms using navigational cues set in the room (Fig. 2*A*). Analysis tracking software was used to determine the number of incorrect arm entries (termed an "error"). The total number of errors before the animal finds the escape platform is used as a metric of learning and memory.

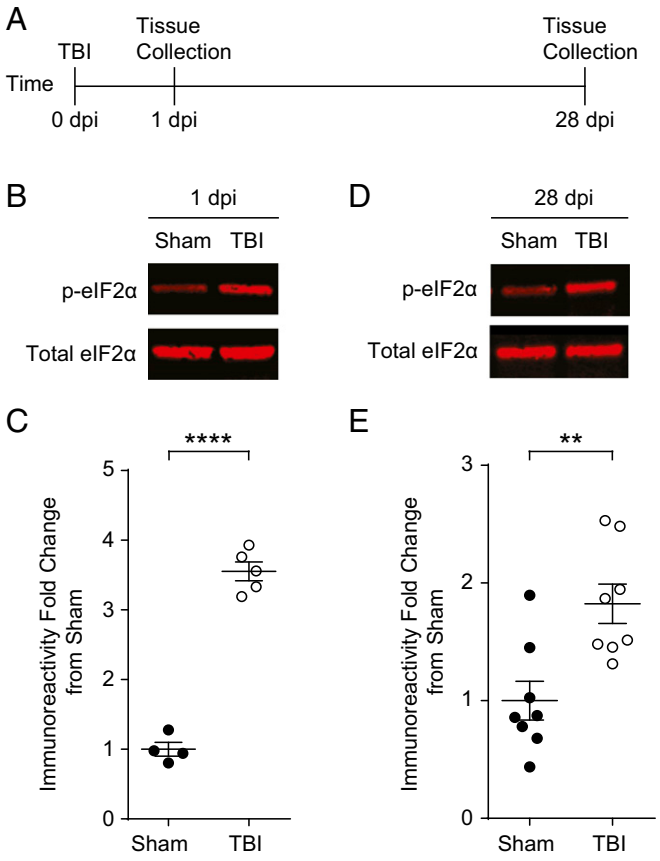

Fig. 1. TBI-induced increase in eIF2α phosphorylation persists 4 wk after injury. (*A*) Experimental design scheme. Animals were given a focal TBI by the controlled cortical impact method and the hippocampus ipsilateral to the injury was collected at either 1 dpi or 28 dpi. Sham controls received a craniectomy without a TBI and were analyzed at the same time points. (*B*) Representative images of p-eIF2α and total eIF2α Western blots from the hippocampi protein samples collected at 1 dpi. (*C*) Quantification of p-eIF2α to total eIF2α ratio normalized to sham. TBI increases phosphorylation of eIF2α at 24 h postinjury. Data are means ± SEM (n = 4–6 per group, Student's t test; ****$P < 0.0001$). (*D*) Representative images of p-eIF2α and total eIF2α. Western blots from the hippocampi collected at 28 dpi. (*E*) Quantification of p-eIF2α to total eIF2α ratio normalized to sham. The increase in p-eIF2α in TBI animals persists at 28 dpi. Data are means ± SEM (n = 8 per group, Student's t test; **$P < 0.01$).

As expected, sham animals learned the location of the escape platform after multiple training blocks (Fig. 2*B*, 28–29 dpi, black solid circles). When memory was measured at 1 d and 7 d after training (Fig. 2*B*, 30 and 37 dpi), sham animals averaged less than one error before locating the escape platform. By contrast, learning was dramatically impaired in mice with TBI, even after multiple training blocks (Fig. 2*B*, 28 dpi, red circles; TBI mice averaged more than three errors). Consequently, when memory was tested on day 30 and day 37, injured mice made significantly more errors compared with sham animals (Fig. 2 *A* and *B*, red solid circles). Thus, these data indicate that TBI impairs learning and memory.

To test whether pharmacological blockage of the ISR restores the lasting learning and memory deficits resulting from TBI, we injected the animals with ISRIB (at 2.5 mg/kg or vehicle) intraperitoneally (i.p.) into both sham and TBI animals. ISRIB treatment started at 27 dpi, the day before the first behavioral training (Fig. 2*B*, 27 dpi), and continued with daily injections throughout the duration of the training (three injections in total, *Materials and Methods*). Strikingly, during training ISRIB-treated injured animals (Fig. 2*B*, 28–29 dpi, red open circles, dotted line) performed better than vehicle-treated TBI animals (Fig. 2*B*, 28–29 dpi, red solid circles). More importantly, memory tested both 1 d (30 dpi) and 7 d (37 dpi) after training was dramatically improved in brain-injured mice treated with ISRB. As ISRIB was given only during training, the data demonstrate that the effect of ISRIB on memory lasts beyond the period of treatment.

ISRIB Reverses TBI-Induced Deficits in Hippocampal Long-Term Potentiation. Sustained changes in synaptic efficacy that result from repeated neuronal activity are believed to constitute the cellular basis of learning and memory (36). The best-characterized form of synaptic plasticity in the mammalian brain is long-term potentiation (LTP), which is manifested as long-lasting increases in synaptic strength. Consistent with the deficits in hippocampal long-term memory, TBI has been previously reported to inhibit hippocampal LTP (37). To examine whether LTP was altered in our focal TBI model, we induced TBI as above, allowed the animals to recover for 4 wk, and measured hippocampal LTP in hippocampal brain slices at Schaffer collateral-CA1 synapses. We observed that LTP was significantly impaired in hippocampal slices from TBI mice compared with those of sham animals (Fig. 3 *A* and *B*). Treatment with ISRIB reversed the deficient LTP in slices from TBI mice (Fig. 3 *A* and *B*). It is noteworthy that ISRIB had no effect on LTP in sham animals (Fig. 3 *A* and *B*), and did not significantly change basal synaptic transmission in TBI mice (Fig. S1). Thus, ISRIB specifically restores LTP in mice with an injured brain. Taken together, these data show that ISRIB restored both hippocampal long-term memory and associated changes in synaptic function in TBI mice.

ISRIB Restores TBI-Induced Deficits in Working and Episodic Learning and Memory in a Concussive Injury Model. To assess the robustness of our results, we next asked whether ISRIB might also be effective in another TBI model. We used a close head injury model (38–40), which mimics diffuse concussive injury commonly observed in human patients (35). Like the focal TBI model, concussive injury resulted in a chronic activation of the ISR in the hippocampus, as determined by increased phosphorylation of eIF2α at 26 dpi (Fig. S2). We evaluated cognitive function using a delayed-matching-to-place paradigm (DMP) (41), a more challenging hippocampal-dependent behavioral task than RAWM. In

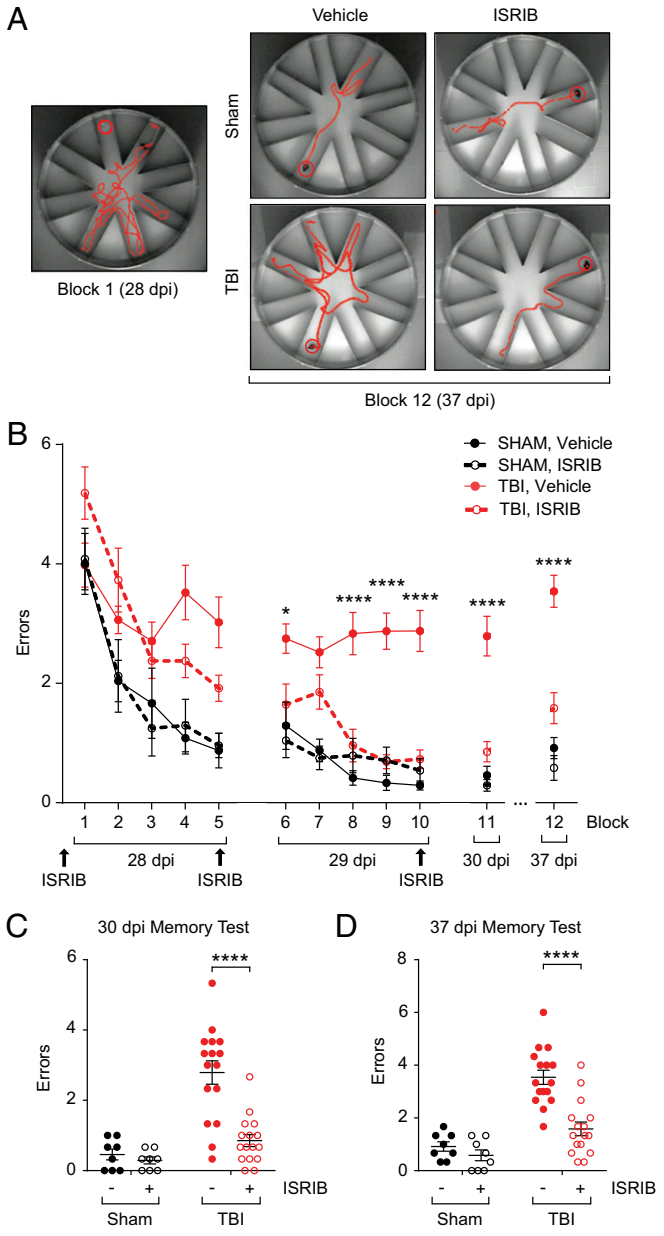

Fig. 2. ISRIB treatment rescues TBI-induced behavioral deficits on the radial arm water maze 28 d after focal TBI. (*A*) Representative track plots showing exploratory activity on the RAWM. Although all animals initially made multiple errors while locating the escape platform (block 1, *Left*), sham and ISRIB-treated TBI animals learned the escape platform location and therefore made fewer errors during the memory test 7 d after training (block 12, 37 dpi). Vehicle-treated TBI animals made more errors than animals in the other three experiment groups (*Right*). (*B*) Animals were i.p. injected (either vehicle or ISRIB) (2.5 mg/kg) the night prior to starting behavior (27 dpi) and after the last trials each day during training (28 and 29 dpi; $n = 8$ per sham group, $n = 16$ per TBI group). Animals ran 15 trials on each training day with the performance of every 3 trials averaged as a single block. Compared with vehicle-treated group (red solid circle, solid line), ISRIB-treated animals (red open circle, dotted line) made significantly less errors over the course of training and when memory was tested 24 hr (30 dpi) and 7 d (37 dpi) after training. Data are means ± SEM (Bonferroni post hoc test, TBI + vehicle vs. TBI + ISRIB; $^{*}P < 0.05$, $^{****}P < 0.0001$). (*C*) Individual animal performance during the memory test 24 h after training (block 11, 30 dpi). Vehicle-treated TBI animals made significantly more errors than all other experimental cohorts. Data are means ± SEM (Bonferroni post hoc test; $^{****}P < 0.0001$). (*D*) Individual animal performance during the memory test 7 d after training (block 12, 37 dpi). Improvement in RAWM performance persisted in ISRIB-treated TBI animals. Data are means ± SEM (Bonferroni post hoc test; $^{****}P < 0.0001$).

DMP, deficits in both working and episodic-like learning and memory are assessed, while eliminating the potential stress-based caveats introduced by water exposure and forced swimming behavior, typically associated with RAWM. Animals on the DMP learn to locate an escape tunnel attached to one of 40 holes in a circular table using visual cues to evade loud noise in a brightly lit room (Fig. 4*A*). Importantly, the escape location was changed every day, forcing the animal to relearn the location of the tunnel. To quantify performance, analysis tracking software measured "escape latency," or the time taken by the mouse to enter the escape tunnel.

Both sham and concussive-injured animals were treated with ISRIB 1 d prior to behavior testing (14 dpi) and after the last trials of each testing day (Fig. 4*B*, 15–17 dpi). Compared with sham, concussive-injured animals failed to learn the task and took significantly longer to reach the escape tunnel (Fig. 4*B*, TBI, vehicle: red solid circles; sham, vehicle: black solid circles), a clear indication that their spatial memory is impaired. By contrast, ISRIB treatment ameliorated the concussive-injured animals' performance by the 3rd and 4th day of testing (Fig. 4B, 17 and 18 dpi; TBI, ISRIB: red open circles, dotted line). Specifically, compared with vehicle-treated injured animals, ISRIB-treated concussive-injured animals, found the escape location faster, on the 3rd and final day of the DMP (Fig. 4 *C* and *D*, 17 and 18 dpi). Thus, ISRIB effectively reversed cognitive deficits induced by a different TBI model and on an additional behavioral task.

Discussion

Our results demonstrate that pharmacological inhibition of the ISR with ISRIB can effectively reverse TBI-induced cognitive deficits in both focal and concussive rodent models. In both injury models, eIF2α phosphorylation was persistently increased, and hippocampus-dependent spatial learning and memory were severely impaired. Remarkably, ISRIB treatment was sufficient to reverse the cognitive deficits in these TBI models. Likewise, LTP was restored in brain slices isolated from brain injured mice when treated with ISRIB. Since the long-term deficits induced by rodent focal contusion injury last for more than a month (as shown here)—and even a year in a corresponding rat model (42)—these results suggest that pharmacological attenuation of the ISR can alleviate TBI-induced dementia and associated changes in synaptic function long after injury.

Unlike previous studies, our work focused on reversal of chronic deficits that develop after TBI. Previous work has been limited to acute injury responses immediately following injury where a robust inflammatory response characterized by immune-cell infiltration into the brain (34, 43–47), cytokine production (39, 40, 48–50), and reactive oxygen species release (51–53) lead to neuronal death. Thus, strategies to counteract acute injury-mediated effects have aimed to dampen the inflammatory response (43, 44, 52, 54, 55). We and others have shown that blocking the acute inflammatory responses within 24 h after injury prevented the development of TBI-induced cognitive deficits (34, 39, 40, 45, 50, 56, 57). However, attempts to translate the insights gleaned from acute TBI models have failed in preclinical studies. In addition, the development of potential treatments that can be effective only within an acute time window after injury poses limitations because their optimal treatment timing may not be feasible in many clinical settings.

In the present study, we demonstrate that treatment with ISRIB at late time points (2 and 4 wk, respectively) rapidly reverses long-term TBI-induced cognitive deficits. Our findings rely on the study of two injury models and combine molecular biology, pharmacology, electrophysiology, and behavioral studies to demonstrate that activation of the ISR is responsible, at least in part, for the memory deficits associated with TBI. As such, our results offer hope that chronic cognitive defects resulting from TBI may be treatable.

Activation of the ISR impairs memory consolidation and activity-dependent changes in synaptic function. Phosphorylation of eIF2α

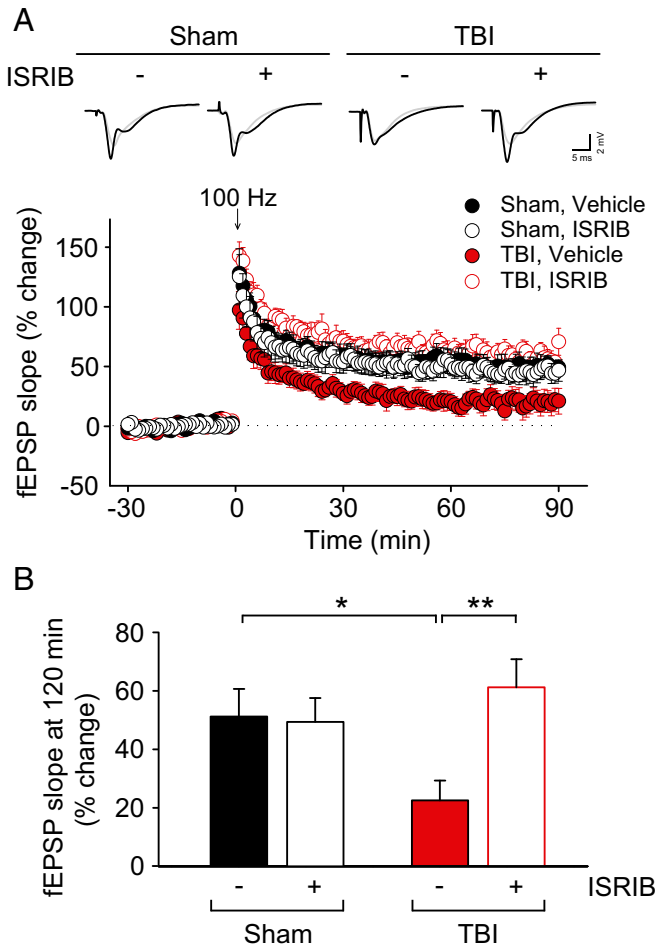

Fig. 3. ISRIB treatment reverses impaired hippocampal LTP in focal TBI mice. (*A, Top*) Representative field excitatory postsynaptic potential (fEPSP) traces at baseline and 90 min after high-frequency stimulation (100 Hz, 1 s). (*Bottom*) LTP was impaired in slices from TBI mice [$F_{(1,12)} = 7.549$, $P = 0.018$; $n = 7$–9 per group], compared with slices from sham mice. ISRIB treatment (50 nM) restored impaired LTP in TBI mice [$F_{(1,14)} = 10.556$, $P = 0.006$], but had no significant effect on LTP in slices from sham mice [$F_{(1,13)} = 0.555$, $P = 0.470$]. Data are means ± SEM (Bonferroni post hoc test; $*P < 0.05$; $**P < 0.01$). (*B*) Summary data show the mean fEPSP slope from 30 min before and 90 min after the stimulation. Data are means ± SEM (Bonferroni post hoc test; $*P < 0.05$; $**P < 0.01$).

inhibits the activity of eIF2's guanine nucleotide exchange factor eIF2B, and ISRIB counteracts this effect by activating eIF2B through dimerization, which renders it less sensitive to inhibition by p-eIF2. The consequences of ISR activation are a general down-regulation of translation of most cellular mRNAs that utilize eIF2 to initiate ribosomes at AUG start codons. In addition, proteins encoded by a small subset of mRNAs that contain strategically placed small open reading frames in their 5′-UTRs become selectively up-regulated when the ISR is activated. ISR-up-regulated proteins include the broadly expressed transcription factor ATF4, a memory repressor gene (58, 59), and the neuronally expressed Rho GAP OPHN1 (33, 60). We have previously shown that eIF2α phosphorylation-mediated increase in OPHN1 leads to AMPA receptor down-regulation and mGluR-induced long-term depression (LTD) in the hippocampus and ventral tegmental area (VTA) (33, 61). We have also found that reduced phosphorylation of eIF2α (or treatment with ISRIB) blocks mGluR-LTD but enhances cocaine-induced LTP in the VTA (61, 62). Whereas it remains unknown whether the principles described for the VTA also apply to the hippocampus, we speculate that ISRIB enhances cognitive abilities by blocking LTD and consequently enhancing LTP, thus keeping synaptic connections stronger. Indeed, reduction of eIF2α phosphorylation enhances hippocampal LTP (19, 22), but blocks mGluR-LTD (33). By contrast, induction of eIF2α phosphorylation in hippocampal neurons impairs LTP (19, 25) and induces mGluR-LTD (33). Thus, our finding that ISRIB treatment rescued long-term TBI-induced deficits in hippocampal LTP is entirely consistent with these studies linking the ISR to LTP.

Most surprisingly, we found that systemic treatment with ISRIB weeks after injury allowed mice to form stable spatial memories that lasted for at least a week even after ISRIB treatment was stopped. ISRIB's bioavailability has a half-life of approximately 8 hr in mouse plasma and in the brain. It equilibrates readily between plasma and the brain and therefore it is entirely cleared from the system within a week (29). Thus, it is highly unlikely that ISRIB is directly influencing memory recall (e.g., Fig. 2, at 37 dpi), but rather that ISRIB has produced enduring changes to memory processes during the treatment period, such as dendritic spine remodeling. Previous work has established that TBI acutely induces significant dendritic spine degeneration (63), and dendritic spine loss persists even a year after a severe TBI (64). In addition, pharmacological induction of eIF2α phosphorylation in chicks blocks training-induced increase in the number of spines in an auditory brain area (24). Given the close association between eIF2α phosphorylation, LTP, and spine formation, the observed lasting effects of ISRIB treatment on memory may point to changes in structural plasticity during learning that persist even in the absence of the ISRIB (65–67).

It remains unclear whether ISRIB is enhancing learning and memory through direct impact on neurons or if the potential therapeutic effects act on other cell types such as microglia, astrocytes, and/or immune cells. Since activation of the ISR and eIF2α phosphorylation causes inflammatory cytokine production (68, 69), and ISRIB interferes with downstream effects of eIF2α, it is possible that ISRIB may be reversing TBI-initiated residual low-grade inflammation that remains after acute inflammation has subsided (34). We have previously shown that pharmacological or genetic blockade of peripherally derived bone marrow macrophage infiltration to the brain ameliorates TBI-induced cognitive loss by preventing inflammatory cytokine production and reactive oxygen species release (34, 53). Whether ISRIB can influence immune cell-mediated cytokine production after TBI is not known. Whereas our previous reports have shown that peripheral macrophage infiltration occurs only acutely after injury, we have observed low-level chronic inflammation after TBI (34). Hence, it is entirely plausible that ISRIB may impact immune function to alleviate cognitive decline.

The surprising results presented here have yet to be extended from mouse models to human physiology. It also remains unclear whether ISRIB treatment cures the cognitive defects permanently or whether lingering pathologies necessitate the ISRIB treatment to be repeated for each new learning task. Chronic activation of the ISR and/or neuroinflammation are associated with numerous neurodegenerative disease states (reviewed in ref. 70). Therefore, increased understanding of these pathways characterized in TBI may have broader therapeutic potential, especially when the window for treating acute injuries has passed. These gaps in our knowledge notwithstanding, we are hopeful that our findings may open promising therapeutic avenues for patients that are suffering from cognitive deficits associated with TBI and other neurodegenerative disorders.

Materials and Methods

Animals. All experiments were conducted in accordance with National Institutes of Health (NIH) *Guide for the Care and Use of Laboratory Animals* (71) and approved by the Institutional Animal Care and Use Committee of the University of California, San Francisco. Male C57B6/J wild-type (WT) mice were purchased from The Jackson Laboratory and used for experiments at

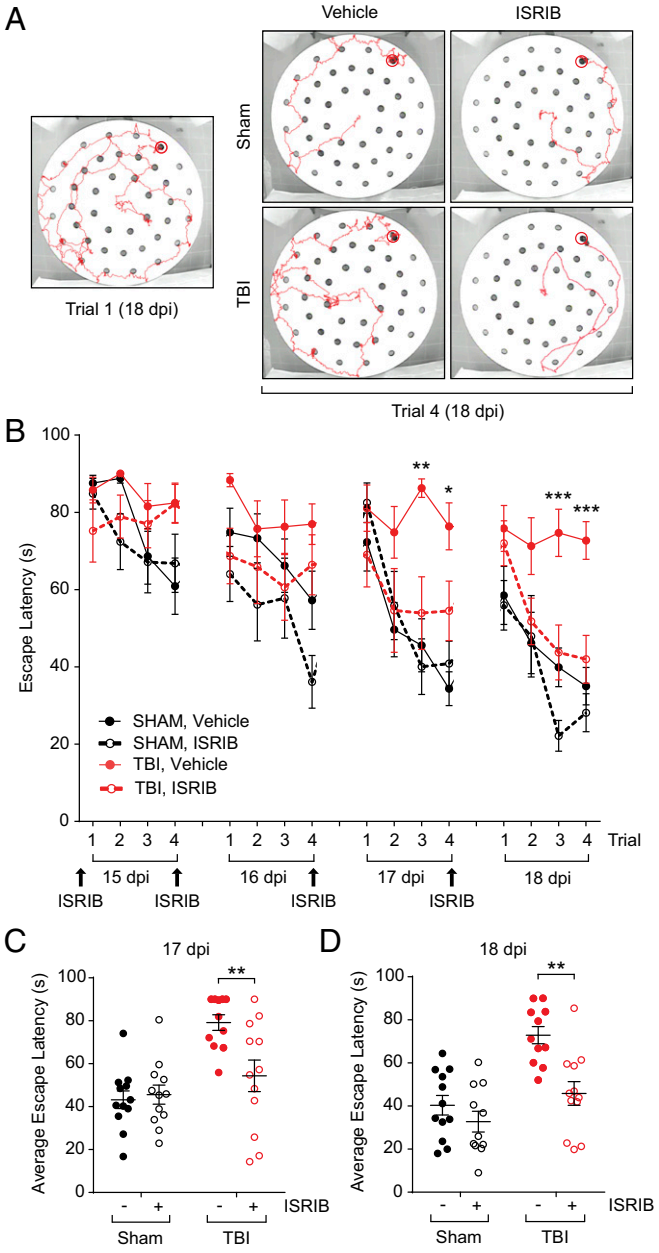

Fig. 4. ISRIB treatment rescues TBI-induced behavioral deficits on the delayed-matching-to-place paradigm 14 d after concussive injury. (*A*) Representative tracks of trials on the modified Barnes maze of the DMP assay. During trial 1 of each day, animals did not know the escape tunnel location and did not find it quickly (trial 1, *Left*). By trial 4, the animals had learned the location of the escape tunnel and took significantly less time on the trial. ISRIB-treated TBI mice showed similar performance as both sham groups on day 4, whereas vehicle-treated TBI mice took longer to escape (*Right*). (*B*) Animals were injected the night before the first day of behavior (14 dpi) and after the last trial of each day (15–17 dpi; $n = 11$–12 per group). Animals that received sham surgeries were able to learn the location of the escape tunnel over the course of each day (vehicle: black solid circle, solid line; ISRIB treated: black open circle, dotted line). TBI animals given vehicle injections (red solid circle, solid line) took longer to find the escape tunnel, whereas TBI animals given ISRIB (red open circle, dotted line) did significantly better than their vehicle-treated counterparts. Data are means ± SEM (Bonferroni post hoc test; $*P < 0.05$, $**P < 0.01$, $***P < 0.001$). (*C*) Individual animal performances averaged across trials 2, 3, and 4 on day 3 of the DMP (17 dpi). TBI animals treated with ISRIB were significantly faster at locating the escape location than their vehicle-treated, TBI counterparts. Data are means ± SEM (Bonferroni post hoc test; $**P < 0.01$). (*D*) Individual animal performances averaged across trials 2, 3, and 4 on day 4 of the DMP (18 dpi). ISRIB-treated TBI animals were significantly faster in locating the escape tunnel than the vehicle-treated TBI group. Data are means ± SEM (Bonferroni post hoc test; $**P < 0.01$).

~12 wk of age. Mice were group housed in environmentally controlled conditions with reverse light cycle (12:12 h light:dark cycle at 21 ± 1 °C) and provided food and water ad libitum.

Surgical Procedure. All animals were randomly assigned to TBI or sham surgeries. Animals were anesthetized and maintained at 2% isoflurane and secured to a stereotaxic frame with nontraumatic ear bars. The hair on their scalp was removed, and eye ointment and betadine were applied to their eyes and scalp, respectively. A midline incision was made to expose the skull.

Focal TBI: Controlled Cortical Impact. A unilateral TBI was induced in the right parietal lobe using the controlled cortical impact model (34). Mice received a ~3.5-mm diameter craniectomy, a removal of part of the skull, using an electric microdrill. The coordinates of the craniectomy were: anteroposterior, −2.00 mm and mediolateral, +2.00 mm with respect to bregma. Any animal that experienced excessive bleeding due to disruption of the dura was removed from the study. After the craniectomy, the contusion was induced using a 3-mm convex tip attached to an electromagnetic impactor (Leica). The contusion depth was set to 0.95 mm from dura with a velocity of 4.0 m/s sustained for 300 ms. These injury parameters were chosen to target, but not penetrate, the hippocampus. Sham animals received craniectomy surgeries but without the focal injury.

Concussive TBI: Closed Head Injury. TBI was induced along the midline of the parietal lobe using the closed head injury model (38). The head of the animal was supported with foam before injury. Contusion was induced using a 5-mm convex tip attached to an electromagnetic impactor (Leica) at the following coordinates: anteroposterior, −1.50 mm and mediolateral, 0 mm with respect to bregma. The contusion was produced with an impact depth of 1 mm from the surface of the skull with a velocity of 5.0 m/s sustained for 300 ms. Any animals that had a fractured skull after injury were excluded from the study. Sham animals received the midline skin incision but no impact.

After focal or concussive TBI surgery, the scalp was sutured and the animal was allowed to recover in an incubation chamber set to 37 °C. Animals were returned to their home cage after showing normal walking and grooming behavior. All animals fully recovered from the surgical procedures as exhibited by normal behavior and weight maintenance monitored throughout the duration of the experiments.

Drug Administration. ISRIB solution was made by dissolving 5 mg ISRIB in 1 mL dimethyl sulfoxide (DMSO) (Fisher Scientific, D128-500) and 1 mL polyethylene glycol 400 (PEG400) (EMD Millipore, PX1286B-2). The solution was gently heated in a 40 °C waterbath and vortexed every 30 s until the solution became clear. The solution was kept in a warm environment throughout the experiment. Each solution was used for injections up to 4 d maximum. If the solution became visibly cloudy or precipitated, a new solution was prepared. ISRIB was delivered at 2.5 mg/kg dosage through i.p. injections. The vehicle solution consisted of 1 mL DMSO and 1 mL PEG400.

Western Blotting. Hippocampi ipsilateral to the TBI in focal injury model animals were removed at 1 or 28 d postsurgery, whereas the right hippocampi from concussive injury model animals were removed at 26 dpi. Samples were processed for protein quantification using homogenization buffer consisting of RIPA lysis and extraction buffer (Fisher Scientific, 89900), PhosSTOP (Roche, 04906845001), and cOmplete ULTRA tablets (Roche, 05892970001). The nuclear and high molecular weight membrane fraction was removed and the remaining cytoplasmic and membrane fraction was quantified through use of a bicinchoninic acid (BCA) assay (Pierce BCA Protein Assay Kit; Fisher Scientific, 23227).

Total protein (50 μg) per lane was loaded onto a 5–15% SDS-polyacrylamide gel (Bio-Rad, 567–1084) for electrophoresis. Proteins were then transferred from gel onto a nitrocellulose membrane for immunodetection. Membranes were blocked for 1 h in 5% nonfat dry milk (NFDM) (Bio-Rad, 170–6404) in PBS with Tween20 (PBS-T) (0.1% Tween20). Antibodies specific for eIF2α (Cell Signaling, 9722; 1:1,000), p-eIF2α (Cell Signaling, 9721; 1:1,000), and GADPH (Sigma, G8795; 1:10,000) were incubated overnight at 4 °C in 5% NFDM in PBS-T. After washes in PBS-T, the membrane was incubated at room temperature for 1 h in appropriate secondary antibodies (Li-Cor) diluted in 1% NFDM in PBST-T. Membranes were scanned using a Li-Cor Odyssey near-infrared imager. Raw

intensity for each band was measured using Li-Cor Odyssey image analysis software. Target protein intensities were normalized to corresponding GADPH loading control intensities to account for amount of protein per well.

Behavioral Assays. For all behavioral assays the experimenters were blinded both to the injury regimen and therapeutic intervention. Behavioral tests were recorded and scored using a video tracking and analysis setup (Ethovision XT 8.5, Noldus Information Technology). Additionally, all behaviors were run on independent animal cohorts.

Radial Arm Water Maze. At 28 dpi, the focal TBI experiment groups ($n = 8$ sham + vehicle, $n = 8$ sham + ISRIB, $n = 16$ TBI + vehicle, and $n = 16$ TBI + ISRIB) were tested on the RAWM assay (34). The maze involved a pool 118.5 cm in diameter with 8 arms, each 41 cm in length, and an escape platform that could be moved (Fig. 1*A*). The pool was filled with water that was rendered opaque by adding white paint (Crayola, 54–2128-053). Visual cues were placed around the room such that they were visible to animals exploring the maze. Animals ran 15 trials a day during training and 3 trials during each memory test. On the first training day, the escape platform could be made visible by placing a flag that could be seen above water on the platform. The escape platform alternated between being visible and hidden for the first 12 trials. The final 3 trials of the first day were all presented with a hidden platform. During the second training day and the memory tests, the escape platform remained hidden. Animals were trained for 2 d and then tested on memory tests 24 h and 7 d after training.

During a trial, animals were placed in a random arm that did not include the escape platform. Animals were allowed 1 min to locate the escape platform. On successfully finding the platform, animals remained there for 10 s before being returned to their holding cage. On a failed trial, animals were guided to the escape platform and then returned to their holding cage 10 s later. The escape platform location was the same, whereas the start arm varied between trials for each individual animal. The escape platform location was randomly assigned for each animal to account for any preferences of exploration in the maze.

Animals were i.p. injected with either vehicle or ISRIB (2.5 mg/kg) starting the day prior to behavior (27 dpi) and after each of the final trials of the training days (28 and 29 dpi) for a total of three injections. No injections were given when memory was tested on days 30 and 37 dpi.

RAWM data were collected through a video tracking and analysis setup (Ethovision XT 8.5, Noldus Information Technology). The program automatically analyzed the number of errors made per trial. Every three trials were averaged into a block to account for large variability in performance; each training day thus consisted of five blocks, whereas each memory test was one block each. Furthermore, the experimenter was blinded to the treatment groups during the behavioral assay.

Delayed-Matching-to-Place Paradigm. At 15 dpi, the concussive TBI experiment groups ($n = 12$ sham + vehicle, $n = 11$ sham + ISRIB, $n = 11$ TBI + vehicle, and $n = 12$ TBI + ISRIB) were tested on DMP using a modified Barnes maze (41). The maze consisted of a round table 112 cm in diameter with 40 escape holes arranged in three concentric rings consisting of 8, 16, and 16 holes at 20, 35, and 50 cm from the center of the maze, respectively. An escape tunnel was connected to one of the outer holes. Visual cues were placed around the room such that they were visible to animals on the table. Bright overhead lighting and a loud tone (2 KHz, 85 db) were used as aversive stimuli to motivate animals to locate the escape tunnel. The assay was performed for 4 d (15–18 dpi). The escape tunnel location was moved for each day and animals ran four trials per day.

During a trial, animals were placed onto the center of the table covered by an opaque plastic box so they are not exposed to the environment. After they had been placed on the table for 10 s, the plastic box was removed and the tone started playing, marking the start of the trial. Animals were given 90 s to explore the maze and locate the escape tunnel. Upon the animals successfully locating and entering the escape tunnel, the tone was stopped. If the animals failed to find the escape tunnel after 90 s, they were guided to the escape tunnel before the tone was stopped. Animals remained in the escape tunnel for 10 s before being returned to their home cage. The maze and escape tunnel were cleaned with ethanol between each trial.

Animals were i.p. injected with either vehicle or ISRIB (2.5 mg/kg) starting the day prior to behavior (14 dpi) and after the final trial of each day (15–17 dpi) for a total of four injections. The experimenter was blind to the treatment groups during the behavioral assay. Each trial was recorded using a video tracking and analysis setup (Ethovision XT 8.5, Noldus Information Technology) and the program automatically analyzed the amount of time required to locate the escape tunnel. The escape latencies of trials 2, 3, and 4 were averaged as a measure of ability to learn and perform the DMP task during the day.

Electrophysiology. Electrophysiological recordings were performed as previously described (22, 72, 73). Briefly, hippocampal slices (350 μm) were cut from brains of sham and TBI (focal injury; $n = 7$–9 per group) mice in 4 °C artificial cerebrospinal fluid (ACSF), kept in ACSF at room temperature for at least 1 hr before recording, and maintained in an interface-type chamber perfused with oxygenated ACSF (95% O_2 and 5% CO_2) containing in millimoles: 124 NaCl, 2.0 KCl, 1.3 $MgSO_4$, 2.5 $CaCl_2$, 1.2 KH_2PO_4, 25 $NaHCO_3$, and 10 glucose (2–3 mL/min). Bipolar stimulating electrodes were placed in the CA1 stratum radiatum to stimulate Schaffer collateral and commissural fibers. Field excitatory postsynaptic potentials (fEPSPs) were recorded using ACSF-filled micropipettes at 28–29 °C. The stimulus strength of the 0.1-ms pulses was adjusted to evoke 30–35% of maximum response. LTP was elicited by a train of high-frequency stimulation (100 Hz, 1 s). When indicated, slices were treated with ISRIB (50 nM) for at least 30 min before stimulation and throughout the entire recording.

Statistical Analysis. All statistical analyses were performed on GraphPad Prism 6 (GraphPad Software). Western blot quantification was analyzed by unpaired Student's *t* test. Behavioral data were analyzed by two-way analysis of variance (ANOVA) with post hoc Bonferroni's multiple comparison. Electrophysiology data were analyzed by one-way ANOVA with post hoc Bonferroni's multiple comparison and n = number of slices. All data presented are means ± SEM with significance set at $P < 0.05$.

ACKNOWLEDGMENTS. We thank Dr. Nicole Day for technical expertise in conducting the initial injury and behavioral experiments; Dr. Carmela Sidrauski, Jordan Tsai, and Aditya Anand for help and advice with drug administration; and Dr. Regis Kelly for invaluable feedback on the manuscript. This work was supported by a generous grant from the Rogers Family Foundation (to S.R. and P.W.) and NIH/National Institute on Aging Grant R21AG042016 (to S.R.). P.W. is an Investigator of the Howard Hughes Medical Institute.

1. Smith DH, Johnson VE, Stewart W (2013) Chronic neuropathologies of single and repetitive TBI: Substrates of dementia? *Nat Rev Neurol* 9:211–221.
2. DeKosky ST, Ikonomovic MD, Gandy S (2010) Traumatic brain injury: Football, warfare, and long-term effects. *N Engl J Med* 363:1293–1296.
3. Sullivan P, Petitti D, Barbaccia J (1987) Head trauma and age of onset of dementia of the Alzheimer type. *JAMA* 257:2289–2290.
4. Engberg AW, Teasdale TW (2004) Psychosocial outcome following traumatic brain injury in adults: A long-term population-based follow-up. *Brain Inj* 18: 533–545.
5. Johnson VE, Stewart W, Smith DH (2010) Traumatic brain injury and amyloid-β pathology: A link to Alzheimer's disease? *Nat Rev Neurosci* 11:361–370.
6. Jellinger KA (2004) Traumatic brain injury as a risk factor for Alzheimer's disease. *J Neurol Neurosurg Psychiatry* 75:511–512.
7. Fleminger S, Oliver DL, Lovestone S, Rabe-Hesketh S, Giora A (2003) Head injury as a risk factor for Alzheimer's disease: The evidence 10 years on; a partial replication. *J Neurol Neurosurg Psychiatry* 74:857–862.
8. Graves AB, et al. (1990) The association between head trauma and Alzheimer's disease. *Am J Epidemiol* 131:491–501.
9. Guo Z, et al. (2000) Head injury and the risk of AD in the MIRAGE study. *Neurology* 54: 1316–1323.
10. Hernandez-Ontiveros DG, et al. (2013) Microglia activation as a biomarker for traumatic brain injury. *Front Neurol* 4:30.
11. Lozano D, et al. (2015) Neuroinflammatory responses to traumatic brain injury: Etiology, clinical consequences, and therapeutic opportunities. *Neuropsychiatr Dis Treat* 11:97–106.
12. Adamides AA, et al. (2006) Current controversies in the management of patients with severe traumatic brain injury. *ANZ J Surg* 76:163–174.
13. Pearn ML, et al. (2017) Pathophysiology associated with traumatic brain injury: Current treatments and potential novel therapeutics. *Cell Mol Neurobiol* 37: 571–585.
14. Harding HP, et al. (2003) An integrated stress response regulates amino acid metabolism and resistance to oxidative stress. *Mol Cell* 11:619–633.
15. Ron D, Harding HP (2012) Protein-folding homeostasis in the endoplasmic reticulum and nutritional regulation. *Cold Spring Harb Perspect Biol* 4:a013177.
16. Donnelly N, Gorman AM, Gupta S, Samali A (2013) The eIF2α kinases: Their structures and functions. *Cell Mol Life Sci* 70:3493–3511.
17. Hinnebusch AG, Ivanov IP, Sonenberg N (2016) Translational control by 5′-untranslated regions of eukaryotic mRNAs. *Science* 352:1413–1416.
18. Sonenberg N, Hinnebusch AG (2009) Regulation of translation initiation in eukaryotes: Mechanisms and biological targets. *Cell* 136:731–745.

19. Costa-Mattioli M, et al. (2007) eIF2alpha phosphorylation bidirectionally regulates the switch from short- to long-term synaptic plasticity and memory. *Cell* 129:195–206.
20. Costa-Mattioli M, Sossin WS, Klann E, Sonenberg N (2009) Translational control of long-lasting synaptic plasticity and memory. *Neuron* 61:10–26.
21. Buffington SA, Huang W, Costa-Mattioli M (2014) Translational control in synaptic plasticity and cognitive dysfunction. *Annu Rev Neurosci* 37:17–38.
22. Zhu PJ, et al. (2011) Suppression of PKR promotes network excitability and enhanced cognition by interferon-γ-mediated disinhibition. *Cell* 147:1384–1396.
23. Stern E, Chinnakkaruppan A, David O, Sonenberg N, Rosenblum K (2013) Blocking the eIF2α kinase (PKR) enhances positive and negative forms of cortex-dependent taste memory. *J Neurosci* 33:2517–2525.
24. Batista G, Johnson JL, Dominguez E, Costa-Mattioli M, Pena JL (2016) Translational control of auditory imprinting and structural plasticity by eIF2α. *eLife* 5:5.
25. Jiang Z, et al. (2010) eIF2alpha Phosphorylation-dependent translation in CA1 pyramidal cells impairs hippocampal memory consolidation without affecting general translation. *J Neurosci* 30:2582–2594.
26. Scheper W, Hoozemans JJ (2015) The unfolded protein response in neurodegenerative diseases: A neuropathological perspective. *Acta Neuropathol* 130:315–331.
27. Petrov T, Underwood BD, Braun B, Alousi SS, Rafols JA (2001) Upregulation of iNOS expression and phosphorylation of eIF-2alpha are paralleled by suppression of protein synthesis in rat hypothalamus in a closed head trauma model. *J Neurotrauma* 18: 799–812.
28. Begum G, et al. (2014) Docosahexaenoic acid reduces ER stress and abnormal protein accumulation and improves neuronal function following traumatic brain injury. *J Neurosci* 34:3743–3755.
29. Sidrauski C, et al. (2013) Pharmacological brake-release of mRNA translation enhances cognitive memory. *eLife* 2:e00498.
30. Sidrauski C, et al. (2015) Pharmacological dimerization and activation of the exchange factor eIF2B antagonizes the integrated stress response. *eLife* 4:e07314.
31. Sekine Y, et al. (2015) Stress responses. Mutations in a translation initiation factor identify the target of a memory-enhancing compound. *Science* 348:1027–1030.
32. Sidrauski C, McGeachy AM, Ingolia NT, Walter P (2015) The small molecule ISRIB reverses the effects of eIF2α phosphorylation on translation and stress granule assembly. *eLife* 4:4.
33. Di Prisco GV, et al. (2014) Translational control of mGluR-dependent long-term depression and object-place learning by eIF2α. *Nat Neurosci* 17:1073–1082.
34. Morganti JM, et al. (2015) CCR2 antagonism alters brain macrophage polarization and ameliorates cognitive dysfunction induced by traumatic brain injury. *J Neurosci* 35:748–760.
35. Xiong Y, Mahmood A, Chopp M (2013) Animal models of traumatic brain injury. *Nat Rev Neurosci* 14:128–142.
36. Neves G, Cooke SF, Bliss TV (2008) Synaptic plasticity, memory and the hippocampus: A neural network approach to causality. *Nat Rev Neurosci* 9:65–75.
37. Schwarzbach E, Bonislawski DP, Xiong G, Cohen AS (2006) Mechanisms underlying the inability to induce area CA1 LTP in the mouse after traumatic brain injury. *Hippocampus* 16:541–550.
38. Webster SJ, Van Eldik LJ, Watterson DM, Bachstetter AD (2015) Closed head injury in an age-related Alzheimer mouse model leads to an altered neuroinflammatory response and persistent cognitive impairment. *J Neurosci* 35:6554–6569.
39. Bachstetter AD, et al. (2015) Attenuation of traumatic brain injury-induced cognitive impairment in mice by targeting increased cytokine levels with a small molecule experimental therapeutic. *J Neuroinflammation* 12:69.
40. Lloyd E, Somera-Molina K, Van Eldik LJ, Watterson DM, Wainwright MS (2008) Suppression of acute proinflammatory cytokine and chemokine upregulation by post-injury administration of a novel small molecule improves long-term neurologic outcome in a mouse model of traumatic brain injury. *J Neuroinflammation* 5:28.
41. Faizi M, et al. (2012) Thy1-hAPP(Lond/Swe+) mouse model of Alzheimer's disease displays broad behavioral deficits in sensorimotor, cognitive and social function. *Brain Behav* 2:142–154.
42. Dixon CE, et al. (1999) One-year study of spatial memory performance, brain morphology, and cholinergic markers after moderate controlled cortical impact in rats. *J Neurotrauma* 16:109–122.
43. Kumar A, Alvarez-Croda DM, Stoica BA, Faden AI, Loane DJ (2016) Microglial/macrophage polarization dynamics following traumatic brain injury. *J Neurotrauma* 33: 1732–1750.
44. Choi BY, et al. (2012) Prevention of traumatic brain injury-induced neuronal death by inhibition of NADPH oxidase activation. *Brain Res* 1481:49–58.
45. Hsieh CL, et al. (2014) CCR2 deficiency impairs macrophage infiltration and improves cognitive function after traumatic brain injury. *J Neurotrauma* 31:1677–1688.
46. Carlos TM, Clark RS, Franicola-Higgins D, Schiding JK, Kochanek PM (1997) Expression of endothelial adhesion molecules and recruitment of neutrophils after traumatic brain injury in rats. *J Leukoc Biol* 61:279–285.
47. Szmydynger-Chodobska J, Strazielle N, Zink BJ, Ghersi-Egea JF, Chodobski A (2009) The role of the choroid plexus in neutrophil invasion after traumatic brain injury. *J Cereb Blood Flow Metab* 29:1503–1516.
48. Acosta SA, Tajiri N, Sanberg PR, Kaneko Y, Borlongan CV (2017) Increased amyloid precursor protein and tau expression manifests as key secondary cell death in chronic traumatic brain injury. *J Cell Physiol* 232:665–677.
49. Acosta SA, et al. (2015) Alpha-synuclein as a pathological link between chronic traumatic brain injury and Parkinson's disease. *J Cell Physiol* 230:1024–1032.
50. Song S, et al. (2016) Granulocyte colony-stimulating factor promotes behavioral recovery in a mouse model of traumatic brain injury. *J Neurosci Res* 94:409–423.
51. Kontos HA (1989) Oxygen radicals in CNS damage. *Chem Biol Interact* 72:229–255.
52. Roth TL, et al. (2014) Transcranial amelioration of inflammation and cell death after brain injury. *Nature* 505:223–228.
53. Morganti JM, et al. (2016) Age exacerbates the CCR2/5-mediated neuroinflammatory response to traumatic brain injury. *J Neuroinflammation* 13:80.
54. Wang GH, et al. (2011) Free-radical scavenger edaravone treatment confers neuroprotection against traumatic brain injury in rats. *J Neurotrauma* 28:2123–2134.
55. Homsi S, et al. (2010) Blockade of acute microglial activation by minocycline promotes neuroprotection and reduces locomotor hyperactivity after closed head injury in mice: A twelve-week follow-up study. *J Neurotrauma* 27:911–921.
56. Acosta SA, et al. (2014) Combination therapy of human umbilical cord blood cells and granulocyte colony stimulating factor reduces histopathological and motor impairments in an experimental model of chronic traumatic brain injury. *PLoS One* 9: e90953.
57. Jacotte-Simancas A, et al. (2015) Effects of voluntary physical exercise, citicoline, and combined treatment on object recognition memory, neurogenesis, and neuroprotection after traumatic brain injury in rats. *J Neurotrauma* 32:739–751.
58. Chen A, et al. (2003) Inducible enhancement of memory storage and synaptic plasticity in transgenic mice expressing an inhibitor of ATF4 (CREB-2) and C/EBP proteins. *Neuron* 39:655–669.
59. Pasini S, Corona C, Liu J, Greene LA, Shelanski ML (2015) Specific downregulation of hippocampal ATF4 reveals a necessary role in synaptic plasticity and memory. *Cell Reports* 11:183–191.
60. Nadif Kasri N, Nakano-Kobayashi A, Van Aelst L (2011) Rapid synthesis of the X-linked mental retardation protein OPHN1 mediates mGluR-dependent LTD through interaction with the endocytic machinery. *Neuron* 72:300–315.
61. Huang W, et al. (2016) Translational control by eIF2α phosphorylation regulates vulnerability to the synaptic and behavioral effects of cocaine. *eLife* 5:5.
62. Placzek AN, et al. (2016) eIF2α-mediated translational control regulates the persistence of cocaine-induced LTP in midbrain dopamine neurons. *eLife* 5:5.
63. Gao X, Deng P, Xu ZC, Chen J (2011) Moderate traumatic brain injury causes acute dendritic and synaptic degeneration in the hippocampal dentate gyrus. *PLoS One* 6: e24566.
64. Ertürk A, et al. (2016) Interfering with the chronic immune response rescues chronic degeneration after traumatic brain injury. *J Neurosci* 36:9962–9975.
65. Kelleher RJ, 3rd, Govindarajan A, Tonegawa S (2004) Translational regulatory mechanisms in persistent forms of synaptic plasticity. *Neuron* 44:59–73.
66. Maletic-Savatic M, Malinow R, Svoboda K (1999) Rapid dendritic morphogenesis in CA1 hippocampal dendrites induced by synaptic activity. *Science* 283:1923–1927.
67. Engert F, Bonhoeffer T (1999) Dendritic spine changes associated with hippocampal long-term synaptic plasticity. *Nature* 399:66–70.
68. Deng J, et al. (2004) Translational repression mediates activation of nuclear factor kappa B by phosphorylated translation initiation factor 2. *Mol Cell Biol* 24: 10161–10168.
69. Zhang K, Kaufman RJ (2008) From endoplasmic-reticulum stress to the inflammatory response. *Nature* 454:455–462.
70. Freeman OJ, Mallucci GR (2016) The UPR and synaptic dysfunction in neurodegeneration. *Brain Res* 1648:530–537.
71. Committee on Care and Use of Laboratory Animals (1996) *Guide for the Care and Use of Laboratory Animals* (Natl Inst Health, Bethesda), DHHS Publ No (NIH) 85-23.
72. Stoica L, et al. (2011) Selective pharmacogenetic inhibition of mammalian target of Rapamycin complex I (mTORC1) blocks long-term synaptic plasticity and memory storage. *Proc Natl Acad Sci USA* 108:3791–3796.
73. Huang W, et al. (2013) mTORC2 controls actin polymerization required for consolidation of long-term memory. *Nat Neurosci* 16:441–448.

Supporting Information

Chou et al. 10.1073/pnas.1707661114

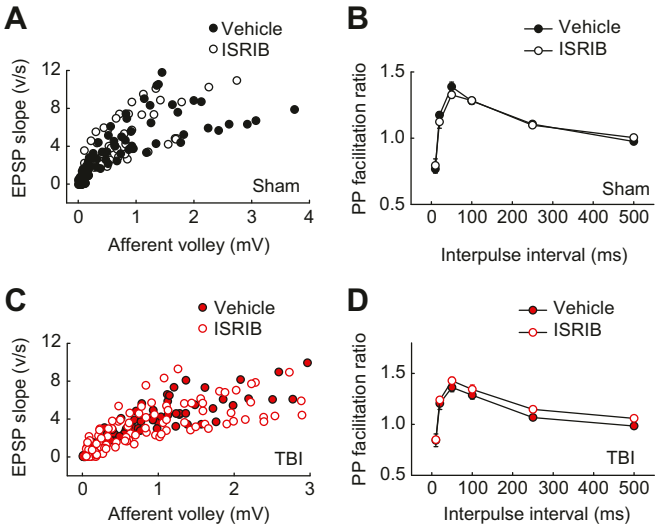

Fig. S1. ISRIB did not alter basal synaptic transmission in hippocampal slices from sham or TBI mice. (*A* and *C*) Input–output plots show similar EPSPs as function of presynaptic fiber volley amplitude over a wide range of stimulus intensities in vehicle-treated and ISRIB-treated slices from sham (*A*; $n = 8$–10 per group) and TBI (C; $n = 11$–13 per group) mice. (*B* and *D*) Paired-pulse facilitation of fEPSPs did not differ between vehicle and ISRIB-treated slices from sham (*B*; $n =$ 6–8 per group) and TBI (*D*; $n = 8$–9 per group) mice, as shown by the plots of the PP ratio ($fEPSP_2/fEPSP_1$) for various intervals of paired stimulation.

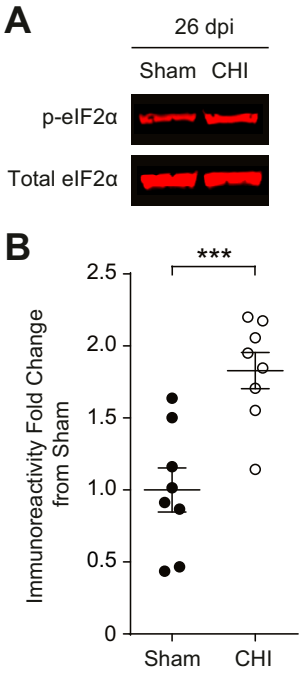

Fig. S2. Closed head injury (CHI) induces an increase in eIF2α phosphorylation. (*A*) Representative images of p-eIF2α and total eIF2α in Western blots from the hippocampi protein samples collected at 26 dpi. (*B*) Quantification of p-eIF2α to total eIF2α ratio normalized to sham. CHI increases phosphorylation of eIF2α at 26 dpi. Data are means ± SEM ($n = 8$ per group; Student's *t* test; $***P < 0.001$).